

PACS numbers: 61.72.Dd, 68.37.Hk, 68.43.-h, 78.30.Hv, 81.05.Rm, 82.30.Vy, 82.75.Fq

Preparation and Characterization of the MCM-41 Nanocatalyst

Jasim Alebrahim, Mohammad Nour Alkhoder, and Reem Tulaimat

*Department of Chemistry,
Albaath University,
Homs, Syria*

In this research scope, the mesoporous nanocatalyst MCM-41 is synthesized using a direct hydrothermal approach. The process initiated with the utilization of sodium metasilicate ($\text{Na}_2\text{SiO}_3 \cdot 5\text{H}_2\text{O}$) as the source of silica and cetyltrimethylammonium bromide (CTAB) playing a pivotal role as a surfactant and template. The hydrothermal reactor is employed, maintaining a temperature of 120°C for the synthesis. The prepared catalysts are characterized through a comprehensive analysis involving Fourier-transform infrared spectroscopy, scanning electron microscopy, and x-ray diffraction. The outcomes of this endeavour yield catalyst particles at the nanoscale, with the majority of them exhibiting dimensions of less than 100 nanometres. Scanning electron microscopy images provide visual evidence of the formation of a uniform and homogeneous mesoporous material. Furthermore, XRD results conclusively verify the attainment of nanoscale dimensions. This achievement is quantitatively determined through the Scherrer equation—a well-established method for estimating crystallite size based on XRD data. This research underscores the successful preparation of MCM-41 nanocatalysts with exceptional mesoporous properties, making them potentially valuable for various applications.

У рамках цього дослідження мезопористий нанокаталізатор MCM-41 був синтезований за допомогою прямого гідротермального підходу. Процес розпочинався з використанням метасилікату Натрію ($\text{Na}_2\text{SiO}_3 \cdot 5\text{H}_2\text{O}$) як джерела кремнезему, а бромід цетилтриметиламонію (СТАВ) відіграв ключову роль як поверхнево-активна речовина та шаблон. Для синтезу використовували гідротермальний реактор, який підтримував температуру у 120°C . Приготовані каталізатори були охарактеризовані шляхом комплексної аналізи, що включає інфрачервону спектроскопію з перетворенням Фур'є, сканувальну електронну мікроскопію та рентгенівську дифракцію. Результати цієї спроби дали нанорозмірні частинки каталізатора, причому більшість із них мали розміри менше 100 нм. Зображення сканувальної електронної мікроскопії надали візуальні докази утворення рівномірного й однорідного мезопо-

ристого матеріалу. Крім того, результати рентгенівської дифракції остаточно підтвердили досягнення нанорозмірів, що було кількісно визначено за допомогою рівняння Шеррера — добре встановленої методи оцінки розміру кристалітів на основі даних рентгенівської дифракції. Це дослідження підкреслює успішне приготування нанокаталізаторів MCM-41 з винятковими мезопористими властивостями, що робить їх потенційно цінними для різних застосувань.

Key words: adsorption, zeolites, mesoporous silica, MCM-41, catalysis.

Ключові слова: адсорбція, цеоліти, мезопористий кремнезем, MCM-41, каталіза.

(Received 19 October, 2023; in revised form, 29 October, 2023)

1. INTRODUCTION

Environmental and economic considerations have garnered increasing interest in restructuring industrial processes in recent years. The aim is to minimize the use of harmful materials and reduce waste. Within this context, heterogeneous catalysis can significantly develop eco-friendly processes in petroleum chemistry and chemical production. Heterogeneous catalysis is distinguished by its ability to separate easily the catalyst from the reactants and its potential for reuse multiple times. Porous materials have been extensively studied and applied in practical applications as catalysts or supports [1]. Porous materials, according to the International Union of Pure and Applied Chemistry (IUPAC), are categorized into three main groups [2]:

1. microporous materials with pore diameters less than 2 nm;
2. mesoporous materials with pore diameters ranging from 2 to 50 nm;
3. macroporous materials with pore diameters larger than 50 nm.

Zeolite, a compound of aluminium silicates, is known for its crystalline structure. It is a type of microporous material that has been extensively studied. Zeolite crystals comprise interconnected three-dimensional frameworks formed by tetrahedral units $[\text{AlO}_4]^{-5}$ and $[\text{SiO}_4]^{-4}$, creating various crystal structures. All of these fall under the chemical category of zeolites [3]. Despite their valuable properties, such as high adsorption capacity and large specific surface area, zeolites have significant application limitations. They cannot effectively accommodate large molecules due to the limited pore sizes, typically ranging from 0.5 to 1.2 nm.

Research has thus been directed towards synthesizing materials structurally similar to zeolites but possessing mesopores with diameters larger than 2 nm. This is crucial to enable the accommodation of larger molecules and expand the potential applications of these

materials [4].

Silicate materials, primarily composed of silicon dioxide (SiO_2), are known for their essential advantages, such as high thermal and chemical stability. These materials do not swell in solvents, making them highly desirable. They find numerous applications in heterogeneous catalysis, adsorption, separation, sensing devices, and removing organic pollutants [2].

Manufacturing porous materials derived from silica has gained significant importance since 1990 after researchers at Mobil Corporation discovered Molecular Sieves of the MMS type. The MCM symbol, 'Mobil Composition of Matter' represents these materials. Several forms of these materials have been synthesized, such as MCM-50 with a layered structure, MCM-48 with a cubic structure, and MCM-41 with a hexagonal shape. All of these materials are essentially composed of (SiO_2) polymeric units [5].

It is worth mentioning that these prepared materials are generally non-crystalline in their overall structure. However, specific order within narrow regions imparts a degree of regularity and organization to them. This results in very sharp peaks in the low-angle X-ray diffraction pattern (less than 10°). The absence of peaks above 10° indicates that the atomic arrangement within the pore walls is in a random and disordered state [6].

MCM-41 has become the most commonly used material due to its flexible synthesis conditions and high specific surface area ($1500 \text{ m}^2/\text{g}$). Additionally, its relatively large pore diameter (2–10 nm) this allows it to absorb a variety of hydrocarbons. It comprises an array of regularly structured hexagonal channels with adjustable sizes, making it versatile for catalysis, adsorption, separation, environmental pollutant removal, and electronic and optical devices [7]. Notably, MCM-41 has been employed as an adsorbent to remove phenol and chlorophenol from wastewater [8].

Nanocatalysts play a crucial role in various chemical applications due to their unique combination of homogeneous and heterogeneous catalysis properties. They offer the advantage of easy separation from the reaction product and possess a high specific surface area. This has led to significant research interest, resulting in various nanostructures, such as nanoclusters, nanospheres, and nanosheets [9, 10]. Therefore, this research paper aimed to synthesize MCM-41 nanocatalysts with nanoscale dimensions.

2. EXPERIMENTS

2.1. Materials

Sodium metasilicate ($\text{Na}_2\text{SiO}_3 \cdot 5\text{H}_2\text{O}$), with a purity of 97% produced

by BDH, was used as the source of silica. Cetyltrimethylammonium bromide (CTAB) ($C_{19}H_{42}BrN$) with a purity of 99%, also from BDH, served as the template. Sulfuric acid (H_2SO_4) was used as a pH-modifying additive with a purity of 97% produced by BDH. Additionally, deionized water was employed as the solvent.

2.2. Preparation of Catalysts

The preparation process of the MCM-41 catalyst involves depositing silica around the micelles formed by the surface-active agent. A solution of cetyltrimethylammonium bromide (CTAB) in deionized water with a concentration of 10% by weight was prepared.

2.5 grams of sodium metasilicate ($Na_2SiO_3 \cdot 5H_2O$) were dissolved in diluted water, and the resulting solution was slowly added to the CTAB solution with vigorous stirring over 2 hours. The pH was adjusted to a value of 11 by adding a 1N sulfuric acid solution. For a further two hours, the mixture was constantly mixed. The resulting solution was transferred to a stainless-steel autoclave lined with Teflon, and it was then heated to $120^\circ C$ and maintained at this temperature for 48 hours under autogenous hydrothermal pressure.

The formed precipitate, primarily consisting of the silica source along with the surface-active agent, was separated, washed with deionized water, and dried at $80^\circ C$ for 24 hours.

Finally, the organic template was removed by calcination in a thermal furnace. The temperature was raised at a rate of $2^\circ C$ per minute from room temperature to $550^\circ C$, and this temperature was maintained for 6 hours.

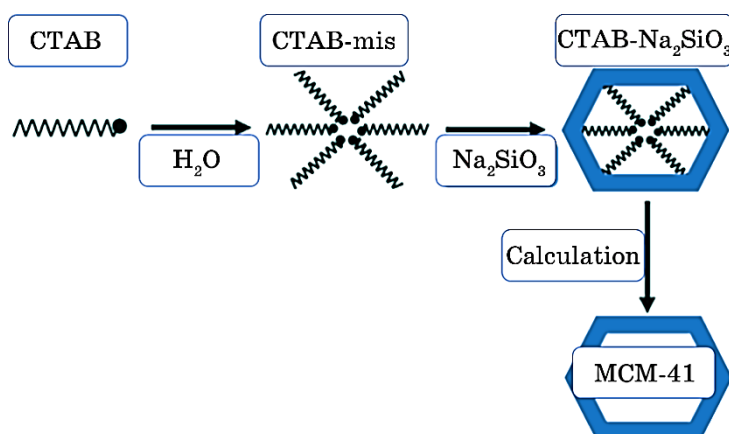


Fig. 1. Diagram for the preparation of MCM-41 catalysts.

3. RESULTS AND DISCUSSION:

3.1. FT-IR

Infrared spectra were recorded using an (FT-IR-4100 type A) instrument from Jasco in the range of $400\text{--}4000\text{ cm}^{-1}$ employing the potassium bromide (KBr) pellet method, commonly used for solid sample analysis. Several milligrams of the MCM-41 catalyst powder were mixed with an equal amount of dry potassium bromide (KBr) powder. The mixture was then ground and transferred to a manual press to create a fragile disk placed in the instrument for spectral recording.

Figure 2 illustrates the resultant absorption spectra of the MCM-41 catalyst before and after calcination. Thus, a distinct and broad absorption band appears at 3450 cm^{-1} , attributed to the asymmetric stretching of the O-H bond in the silanol Si-OH groups and water molecules (H-O-H). Another band at 1635 cm^{-1} corresponds to the bending vibration of water molecules. The bands at 1081 cm^{-1} and 804 cm^{-1} are related to the symmetric and asymmetric stretching of the Si-O-Si bond, respectively. Finally, the band at 456 cm^{-1} indicates the bending vibration of the Si-O bond [6, 7, 11].

3.2. SEM Analysis

It is a type of electron microscopy that generates detailed images of a sample by scanning its surface with a focused beam of high-energy electrons. These electrons interact with the atoms in the sample, producing various signals containing information about

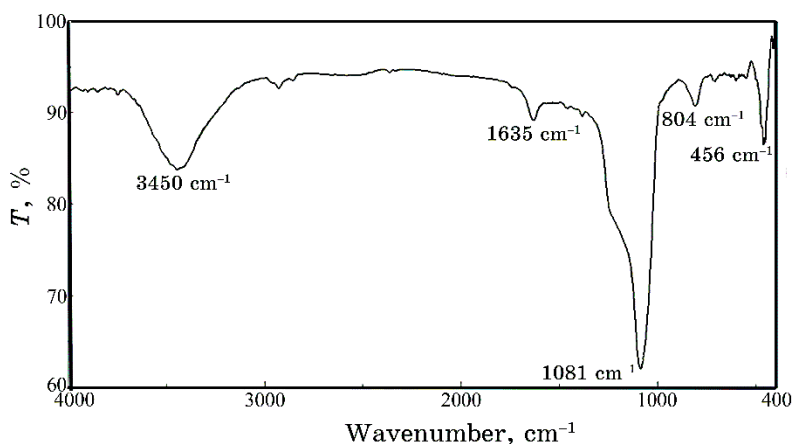


Fig. 2. Infrared spectrum of the calcined MCM-41 catalyst.

surface topography and sample composition. The electron beam is scanned in a point-by-point raster pattern, and the beam's position is correlated with the intensity of the detected signal to create an image.

Figure 3 illustrates scanning electron microscopy (SEM) images of the prepared catalyst. As shown in Figure 4, the SEM image of

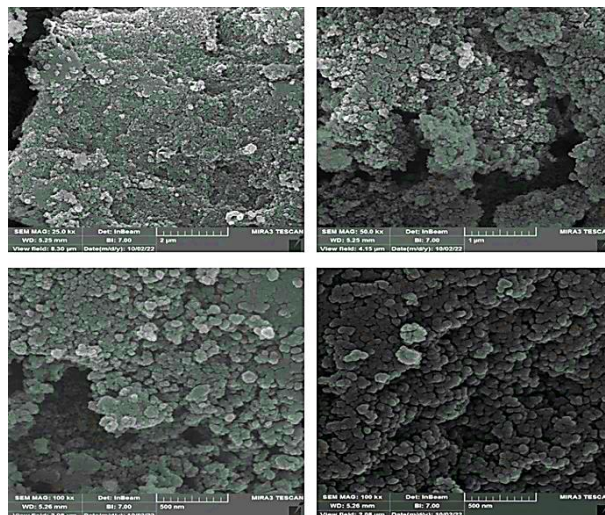


Fig. 3. Scanning electron microscopy (SEM) images of the MCM-41 material.

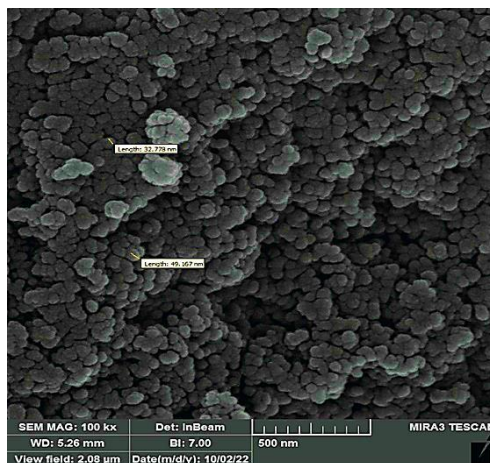


Fig. 4. The scanning electron microscopy (SEM) image of the MCM-41 material with nanoscale dimensions.

the catalyst reveals that most of the particles are relatively small, individual, and have dimensions within the range of approximately 30–50 nm. They exhibit a regular spherical shape, high homogeneity, and distinctiveness among the particles.

3.3. XRD Analysis

Figure 5 show the pattern XRD of the prepared and calcinated MCM-41 sample at 550°C for 6 hours, within the 2θ range of 1–10°, revealing a prominent and robust peak (d_{100}) at $2\theta = 1.1^\circ$ calculations were performed to determine the dimensions of the resulting crystals using Scherrer equation [12].

$$D = \frac{K\lambda}{\beta_{FWHM} \cos \theta},$$

where K is a constant with a value of 0.94, λ —x-ray wavelength used in XRD and its value of 0.1540 nm for the copper element, β_{FWHM} —the peak width at half maximum is measured in radians, and (D) represents the crystal dimensions in nanometres, θ —x-ray diffraction angle.

The calculated and measured values in Table confirm the

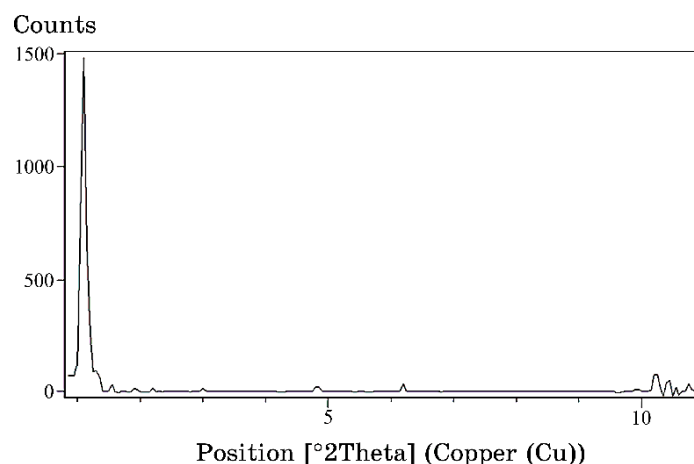


Fig. 5. X-ray diffraction pattern of calcinated MCM-41 catalyst.

TABLE. Results of XRD data for MCM-41 catalyst.

2θ	θ , rad	$FWHM$	β_{FWHM}	D , nm
1.1	0.009599	0.2131	0.003719	38.9397

achievement of nanoscale dimensions. By examining the values D , we find that the prepared catalyst MCM-41 has nanoscale dimensions, with particle size in the order of 38.9397 nm. This is consistent with the results obtained from the scanning electron microscope. This will enhance its catalytic effectiveness in various chemical and industrial applications.

4. CONCLUSIONS

In this research, nanoscale silica-based MCM-41 catalysts were prepared. The electron microscopy images confirmed the nanoscale structure of the prepared catalyst, with an average particle size ranging from approximately 30–50 nm. X-ray diffraction results indicated the nanoscale dimensions, with a particle size of about 39 nm. These characteristics enhance their catalytic efficiency for various chemical and industrial applications.

REFERENCES

1. A. Taguchi and F. Schüth, *Microporous Mesoporous Mater.*, **77**, Iss. 1: 1 (2005); <https://doi.org/10.1016/j.micromeso.2004.06.030>
2. B. Zdravkov, J. Čermák, M. Sefara, and J. Janků, *Cent. Eur. J. Chem.*, **5**, Iss. 2: 385 (2007); <https://doi.org/10.2478/s11532-007-0017-9>
3. T. Armbruster and M. E. Gunter, *Rev. Mineral. Geochem.*, **45**, Iss. 1: 1 (2001); <https://doi.org/10.2138/rmg.2001.45.1>
4. G. Øye, W. R. Glomm, T. Vrelstad, S. Volden, H. Magnusson, M. Stöcker, and J. Sjöblom, *Adv. Colloid Interface Sci.*, **123**, Iss. 1: 17 (2006); <https://doi.org/10.1016/j.cis.2006.05.010>
5. M. B. Bahari, S. N. Bukhari, L. N. Jun, and H. D. Setiabudi, *Mater. Today*, **42**, Iss. 1: 33 (2021); <https://doi.org/10.1016/j.matpr.2020.09.144>
6. D. S. Lee and T. K. Liu, *J. Sol-Gel Sci. Technol.*, **24**, Iss. 1: 69 (2002); <https://doi.org/https://doi.org/10.1023/A:1015165600804>
7. K. Wu, B. Li, C. Ha, and J. Liu, *Appl. Catal. A*, **479**, Iss. 5: 70 (2014); <https://doi.org/10.1016/j.apcata.2014.04.004>
8. P. A. Mangrulkar, S. P. Kamble, J. Meshram, and S. S. Rayalu, *J. Hazard. Mater.*, **160**, Iss. 2–3: 414 (2008); <https://doi.org/10.1016/j.jhazmat.2008.03.013>
9. S. Oliveira, S. P. Forster, and S. Seeger, *J. Nanotechnol.*, **2014**, Iss. 3: 1 (2014); <https://doi.org/10.1155/2014/324089>
10. A. Zuliani, F. Ivars, and R. Luque, *Chem. Cat. Chem.*, **10**, Iss. 9: 1968 (2018); <https://doi.org/10.1002/cctc.201701712>
11. R. K. Rana and B. Viswanathan, *Catal. Lett.*, **52**, Iss. 1: 25 (1998); <https://doi.org/10.1023/A:1019019403375>
12. T. S. Reddy and M. C. S. Kumar, *Ceram. Int.*, **42**, Iss. 10: 12262 (2016); <https://doi.org/10.1016/j.ceramint.2016.04.172>